Supplementary Information for

ERK1/2-dependent activation of FCHSD2 drives cancer cell-selective regulation of clathrin-mediated endocytosis

Guan-Yu Xiao, Aparna Mohanakrishnan and Sandra L. Schmid

Sandra L. Schmid
Email: Sandra.schmid@utsouthwestern.edu

This PDF file includes:

> SI Materials and Methods
> Figs. S1 to S7
> Table S1
> Captions for database S1

Other supplementary materials for this manuscript include the following:

> Dataset S1

SI Materials and Methods

      Immunoprecipitation, Mass Spectrometry and Proteomic Analysis. HCC4017 stably expressing FCHSD2-Myc were washed three times with PBS and starved in RPMI 1640 without FCS for 16 h. The cells then were untreated or treated with 100 ng/ml of EGF for 10 min. After the EGF treatment, cells were washed three times with PBS and lysed for 30 min at 4°C in lysis buffer (20 mM HEPES (pH 7.4), 150 mM KCl, 2 mM MgCl$_2$, 1 mM Na$_3$VO$_4$, 1X Protease Inhibitor Cocktail, 1X Phosphatase Inhibitor Cocktail) containing 0.2% Triton X-100. Lysates were clarified at 12,000g for 15 min at 4°C. After quantification using BCA method (Thermo Fisher Scientific), about 3 mg of total protein lysate in 500 µl lysis buffer was used for each immunoprecipitation. Anti-Myc-DDK antibody (#TA50011-100, OriGene) was used to immunoprecipitate FCHSD2-Myc by incubation with the lysate for 1 h at 4°C. Addition of Protein G beads (approximately 40 µl) (MilliporeSigma) in the lysate followed by gentle rotation for 1 h at 4°C allowed binding of target proteins. Beads were washed three times in lysis buffer and then denatured using reducing Laemmli sample buffer, boiled and run on SDS-PAGE gel.

      Protein gel pieces was reduced and alkylated with DTT (20 mM) and iodoacetamide (27.5 mM). A 0.01 µg/µl solution of trypsin in 50 mM triethylammonium bicarbonate (TEAB) was added to completely cover the gel, allowed to sit on ice, and then 50 µl of 50 mM TEAB was added and the gel pieces were digested overnight (Pierce). Following solid-phase extraction cleanup with an Oasis HLB µelution plate (Waters), the resulting peptides were reconstituted in 10 ul of 2% (v/v) acetonitrile (ACN) and 0.1% trifluoroacetic acid in water. Five ul of this were injected onto an Orbitrap Fusion Lumos mass spectrometer (Thermo Electron) coupled to an Ultimate 3000 RSLC-Nano liquid chromatography systems (Dionex). Samples were injected onto a 75 µm i.d., 50-cm long EasySpray column (Thermo), and eluted with a gradient from 1-28% buffer B over 60 min. Buffer A contained 2% (v/v) ACN and 0.1% formic acid in water, and buffer B contained 80% (v/v) ACN, 10% (v/v) trifluoroethanol, and 0.1% formic acid in water. The mass spectrometer operated in positive ion mode with a source voltage of 2.4 kV and an ion transfer tube temperature of 275 °C. MS scans were acquired at 120,000 resolution in the Orbitrap and up to 10 MS/MS spectra were obtained in the Orbitrap for each full spectrum acquired using higher-energy collisional dissociation (HCD) for ions with charges 2-7. Dynamic exclusion was set for 25 s after an ion was selected for fragmentation.

      Raw MS data files were analyzed using Proteome Discoverer v2.2 (Thermo), with peptide identification performed using Sequest HT. Fragment and precursor tolerances of 10 ppm and 0.6 Da were specified, and three missed cleavages were allowed. Carbamidomethylation of Cys was set as a fixed modification. Oxidation of Met and phosphorylation of Ser, Thr, and Tyr were also set as variable modifications and were localized using ptmRS.
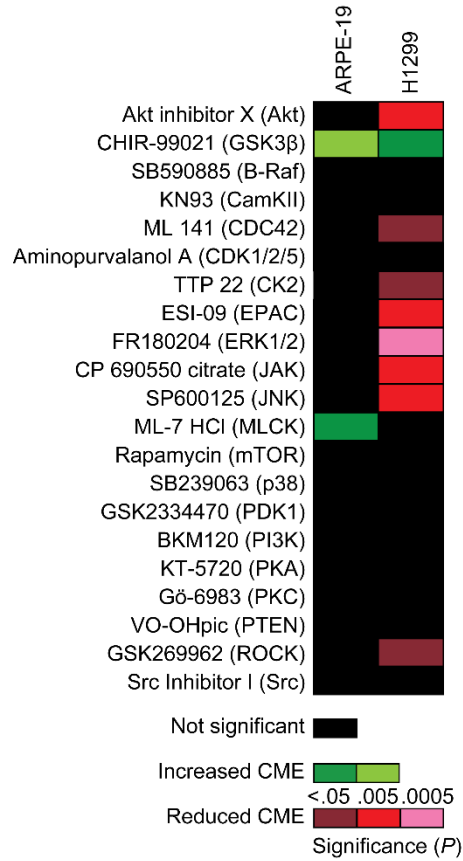
Fig. S1. Analysis of the effects of kinase inhibitors on the endocytosis of TfnR in human non-cancerous ARPE-19 and H1299 NSCLC cells. Heatmap illustrating the effects of the indicated inhibitors on TfnR endocytosis in non-cancerous ARPE-19 cells and H1299 NSCLC cells.
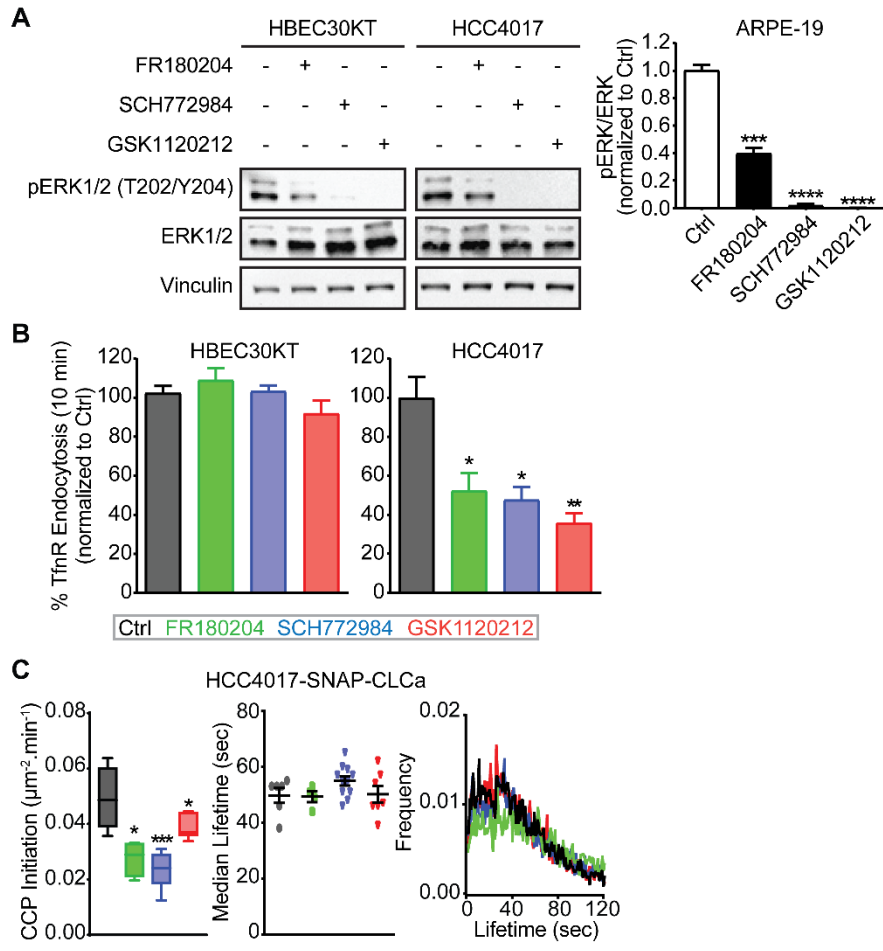
Fig. S2. ERK1/2 specifically affects CME activities in cancer cells. (*A*) Representative western blots to measure the efficiencies of kinase inhibitors in reducing ERK1/2 phosphorylation in control, ERK1/2 inhibitor (FR180204 and SCH772984, 10 μM)-treated or MEK1/2 inhibitor (GSK1120212, 10 μM)-treated HBEC30KT and HCC4017 cells. Quantification of pERK/ERK intensity ratios in ARPE-19 cells treated with the indicated inhibitors, corresponding to Fig. 2*A*. All data were normalized to control and represent mean ± SEM (*n* = 3). (*B*) Endocytosis of TfnR was measured in HBEC30KT and HCC4017 cells either untreated (Ctrl) or treated with the indicated inhibitor. All data were normalized to control and represent mean ± SEM (*n* = 3). (*C*) Rates of initiation (no. CCPs·μm^2·min) (*Left*), median lifetime (*Middle*) and average lifetime distributions (*Right*) of bona fide CCPs in control and inhibitor-treated HCC4017 cells. Data were obtained from at least 15 cells/condition (>10,000 CCPs/condition), the box plots represent median, 25th and 75th percentiles, and outermost data points. Two-tailed Student's *t* tests were used to assess statistical significance for comparison with Ctrl. *P < 0.05, **P < 0.005, ***P < 0.0005, ****P < 0.00005.
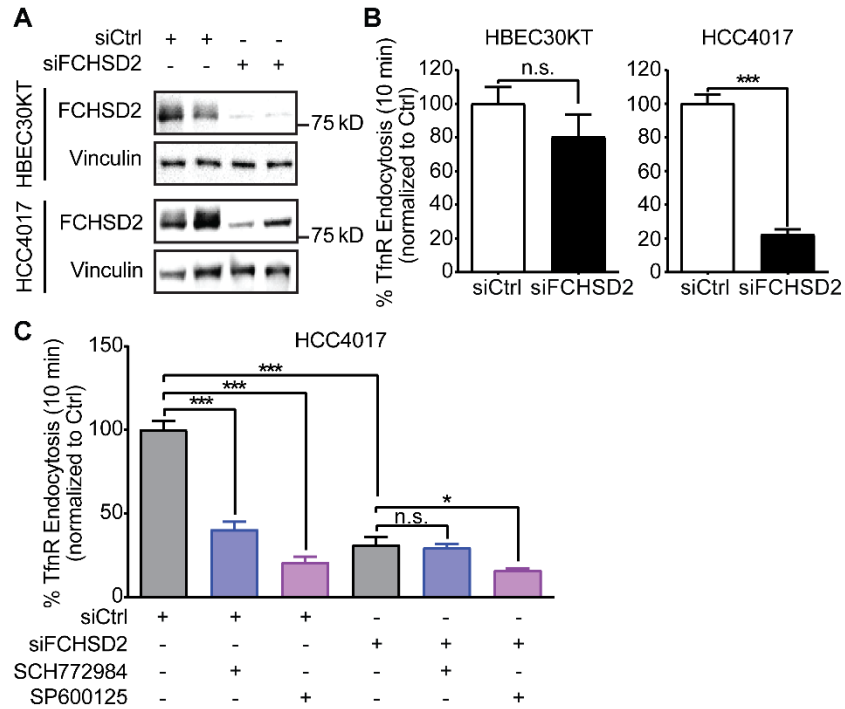
Fig. S3. FCHSD2 is specifically required for CME in cancer cells. (*A*) Representative western blots and the quantification of FCHSD2 knockdown efficiency in control and FCHSD2 siRNA-treated HBEC30KT and HCC4017 cells. (*B*) Endocytosis of TfnR was measured in control and FCHSD2 siRNA-treated HBEC30KT and HCC4017 cells. All data were normalized to control. (*C*) Endocytosis of TfnR was measured, as described in (*B*), in control and FCHSD2 siRNA-treated HCC4017 cells in the absence or presence of the ERK1/2 inhibitor SCH772984 (10 μM) or the JNK inhibitor SP600125 (10 μM). All data represent mean ± SEM (*n* = 3). Two-tailed Student's *t* tests were used to assess statistical significance for the indicated dataset. n.s., not significant, *$P < 0.05$, ***$P < 0.0005$.
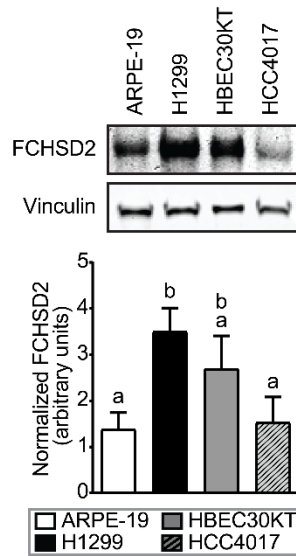
Fig. S4. FCHSD2 expression varies between cell lines. Representative western blots of FCHSD2 and the quantification of normalized FCHSD2 expression levels (FCHSD2/Vinculin intensity ratios) in ARPE-19, H1299, HBEC30KT and HCC4017 cells. Data represent mean ± SEM (n = 3). ANOVA followed by Tukey's pairwise test was used to assess statistical significance among different datasets. Values bearing the same letter (a or b) are not significantly different from each other. Values labeled 'b' are significantly different from values labeled 'a' ($P < 0.05$).
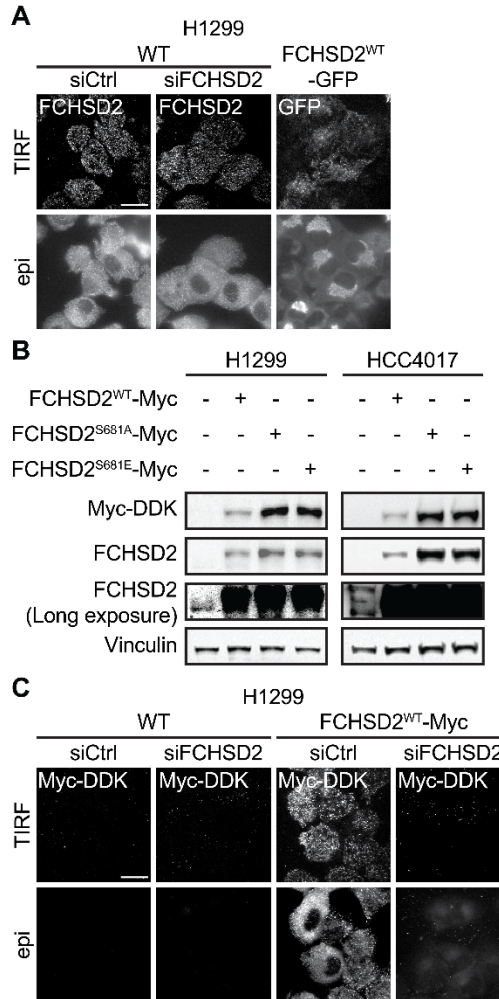
Fig. S5. Specificity of commercially available FCHSD2 and Myc-DDK antibodies for immunolocalization. (*A*) Representative TIR-FM and epi images of FCHSD2 immunofluorescence staining detected with α-FCHSD2 antibody (#PA5-58432) in control (left panel) and FCHSD2 siRNA-treated (middle panel) H1299 cells. siRNA-mediated knockdown of FCHSD2 did not alter the nonspecific staining observed. Images for FCHSD2^{WT}-GFP transduced H1299 cells (right panel) showing perinuclear aggregation. Scale bar, 25 μm. (*B*) Representative western blots used to test the specificity of Myc-DDK antibody in FCHSD2^{WT}-Myc, FCHSD2^{S681A}-Myc, or FCHSD2^{S681E}-Myc transduced H1299 and HCC4017 cells. (*C*) Representative TIR-FM and epi images of Myc-DDK immunofluorescence staining in control and FCHSD2 siRNA-treated WT or FCHSD2^{WT}-Myc transduced H1299 cells, demonstrating specificity of this antibody. Scale bar, 25 μm.
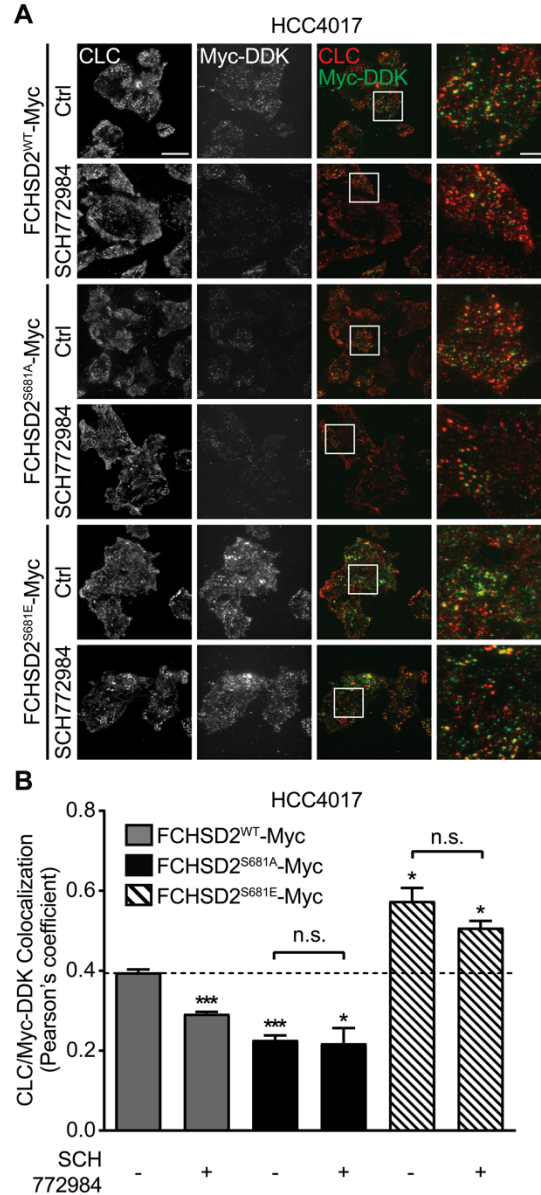
Fig. S6. ERK1/2 activity regulates FCHSD2 recruitment to the plasma membrane and CCPs. (*A*) Representative TIR-FM images of CLC and Myc-DDK immunofluorescence staining in FCHSD2^{WT}-Myc, FCHSD2^{S681A}-Myc, or FCHSD2^{S681E}-Myc transduced HCC4017 cells in the absence or presence of the ERK1/2 inhibitor SCH772984 (10 μM). (Scale bars: 25 μm in overviews, 6.25 μm in the magnified views at far right.) (*B*) Colocalization of CLC and Myc-DDK immunofluorescence staining in the cells as described in (*A*). Data were obtained from n = 3 independent experiments, at least 40 cells in total/condition and represent mean ± SEM. Two-tailed Student's *t* tests were used to assess statistical significance for comparison with FCHSD2^{WT}-Myc without SCH772984 treatment and for the indicated dataset. n.s., not significant, *$P < 0.05$, ***$P < 0.0005$.
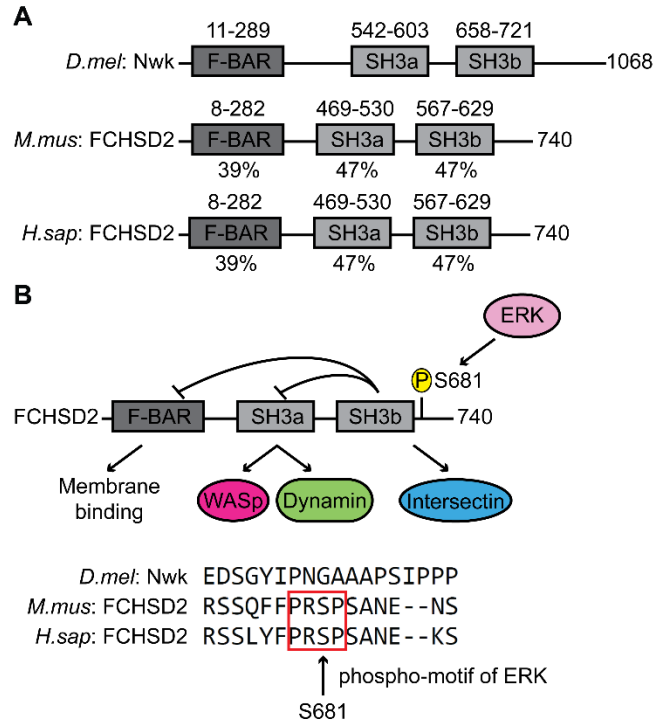
Fig. S7. Mammalian FCHSD2 is homologous to fly Nwk and phosphorylated by ERK1/2 kinases. (*A*) Schematic drawing of the domain structures of *Drosophila melanogaster* Nwk, *Mus musculus* and *Homo sapiens* FCHSD2. (*B*) Model of the ERK-mediated phosphorylation site in autoregulated FCHSD2 and the interactions between FCHSD2, WASp, dynamin, and intersectin. The phosphorylation site in mammalian FCHSD2 is not conserved in Nwk.

Table S1. Post-translational modification (PTM) sites in human FCHSD2 identified by proteomic analysis.

HCC4017 cells transfected with FCHSD2-Myc

The cells were starved in RPMI 1640 without serum for 16 h

Confidence	Peptide Sequence	Modifications	Site (Human)
High	SFLEGTMQVAQSR	1xOxidation	M95
High	MNICENYK	1xOxidation;	M102; C105
		1xCarbamidomethyl	
High	CVDQLTK	1xCarbamidomethyl	C130
High	KYFETEQMAHAVR	1xOxidation	M161
High	YYQTDLVNIMK	1xOxidation	M234
High	VLNDLECHGAAVSEQSR	1xCarbamidomethyl	C378
High	SAMNQVMEELENER	2xOxidation	M410; M414
High	SHTSSNSTEAELVSGSLNGDASVCFVK	1xCarbamidomethyl	C570

After serum starvation for 16 h, the cells were treated with EGF (100 ng/ml) for 10 min

Confidence	Peptide Sequence	Modifications	Site (Human)
High	SMYPVWK	1xOxidation	M83
High	SFLEGTMQVAQSR	1xOxidation	M95
High	MNICENYK	1xOxidation;	M102; C105
		1xCarbamidomethyl	
High	CVDQLTK	1xCarbamidomethyl	C130
High	KYFETEQMAHAVR	1xOxidation	M161
High	TELETCQAVQNTFQFLLENSSK	1xCarbamidomethyl	C260
High	DYNLQLFLQENAVFHKPQPFQFQPCDSDTSR	1xCarbamidomethyl	C304
High	SAMNQVMEELENER	2xOxidation	M410; M414
High	NYPLTCK	1xCarbamidomethyl	C474
High	YLQFPTSNSLLSMLQSLAALDSR	1xOxidation	M536
High	SHTSSNSTEAELVSGSLNGDASVCFVK	1xCarbamidomethyl	C570
High	SSLYFPRSPSANEK	1xPhospho	S681*

Master Protein Accessions: O94868. * indicates the EGF-dependent phosphorylation site.

Additional data table S1 (separate file)

Dataset S1. WB quantification for Fig. 7*A*, corresponding to Fig. 7*B*.